



OPEN

Hydrogeochemical factors influencing the dynamics of groundwater characteristics in eco-sensitive areas of the Southern Western Ghats, India

Pankaj Bakshe^{1✉}, Mini Chandran¹, Bindu J. Viju¹, Aneesh Kumar Narikkatan¹ & Ravin M. Jugade²

The inter-ionic relationships of groundwater present in a region as well as various chemical and physical factors all have an impact on the geochemistry of groundwater in an aquifer. To assess the factors influencing the geochemical composition of groundwater in the eco-sensitive area of Western Ghats, Kerala, India, various weathering, and ionic indices were analyzed. Results show groundwater ranges from soft to extremely hard and acidic to alkaline, with high Mn and Fe levels. WQI analysis found 7% of samples unfit for drinking due to Fe/Mn contamination in the southeast part of the study area. Main water types are CaHCO₃ (46%) and CaMgCl. Geochemical modeling indicates silicate and carbonate weathering, cation exchange, and reverse ion processes influence the aquifer. Groundwater is often supersaturated with iron minerals, saturated with carbonate minerals, and undersaturated with sulfate and chloride minerals. Cluster analysis (CA) revealed that NO₃⁻ and K⁺ are derived from anthropogenic sources. Principal component analysis (PCA) resulted in three factors. Factor 1 is for geogenic processes, while Factors 2 and 3 imply the anthropogenic and weathering of iron-rich minerals. Hierarchical cluster analysis defines anthropogenic input, silicate and carbonate weathering, and different patterns of mineralization in the groundwater. The study underscores the need for comprehensive management to protect groundwater quality, considering the complex interplay of natural processes and human factors.

Keywords Groundwater, Water quality index, Saturation index, Geochemical weathering, Polar heatmap cluster

As a significant natural resource, groundwater is required to sustain all forms of life on Earth due to its natural purity and status as one of the most significant sources of pure water on the surface of the planet^{17,21,42,48}. The quality of groundwater and its applications are primarily influenced by several variables, including the overall condition of the sub-surface environment, the composition of lithological formations, hydro geochemical interactions occurring within the aquifer, and numerous human activities^{3,27,62}. The identification of sources of groundwater chemistry is of utmost importance in the context of addressing issues related to water supply–demand dynamics and socio-economic development, particularly in the face of challenges like as overexploitation and droughts resulting from climate change¹⁵. The chemical composition of groundwater is typically subject to various influences, including precipitation patterns, geological formations, rock types, and the duration of residence along the flow paths of groundwater^{19,28,38}.

According to the 6th Minor Irrigation Census, India is the world's largest extractor of groundwater, withdrawing over 250 cubic kilometers annually, which is about 25% of the global total. Groundwater is crucial for India, supplying 62% of irrigation, 85% of rural water, and 50% of urban water. Moreover, it is worth noting that

¹Central Ground Water Board, Kerala Region, Trivandrum 695004, India. ²Department of Chemistry, RTM Nagpur University, Nagpur 440033, India. ✉email: pankajbakshe@gmail.com

in the nation of India, there exist expansive mountainous and hilly regions, which account for approximately 30% of the total land area. These topographical features play a crucial and noteworthy role in the supply of water resources to the nation. This is primarily due to their unique characteristics, including heightened precipitation levels compared to lowland regions, reduced evapotranspiration rates at higher elevations, and substantial water reservoirs in various forms⁵³. The Western Ghats, a mountain range running parallel to India's western coast 30–50 km inland, covers about 140,000 km² and stretches 1600 km. It extends from the northern Satpura Range through Goa, Karnataka, Kerala, and Tamil Nadu, ending at Kanyakumari, where it embraces the Indian Ocean. Therefore, it is equally crucial to examine groundwater hydrochemistry in this area.

The two main challenges pertaining to groundwater are issues of water scarcity and water quality. The severity of these issues varies greatly and is directly correlated to the geology, hydrogeology, climate, and geochemical mechanisms. The chemical composition of groundwater is influenced by many key factors, including the quality and quantity of recharged water, the geologic structure, and the mineralogy of the aquifer⁶⁸. According to the findings of the hydrochemical studies, the quality of groundwater is dependent on lithological and pedo-geochemical compositions, as well as numerous geochemical compositions of the rocks and anthropogenic activities^{2,26,49}. Groundwater chemistry may be affected by a variety of anthropogenic causes, including waste disposal approaches and sanitary conditions. Lithology and geochemistry can potentially modify groundwater hydrochemical characteristics through subsurface movement^{6,15,49,58,59,67}. Comprehending the quality of groundwater and its underlying mechanisms is of utmost importance in order to facilitate efficient management and ensure the long-term sustainability of this vital resource for many applications. The chemical composition of groundwater is influenced by several geochemical processes that occur throughout its flow. Therefore, accurately identifying the aquifer's location is crucial in order to understand the dispersion and mechanisms of the dominant ion chemistry within the area^{25,56}. The groundwater chemistry of an area is typically not homogeneous, being affected by factors such as flow, geochemical processes, evaporation, evapotranspiration, and possible pollution sources^{55,58}. The comprehension of many interconnected geochemical processes is crucial for comprehending the underlying factors contributing to changes in water quality resulting from aquifer interaction, particularly in formations characterized by weathered rock. Hydrogeochemical techniques may be used for the purpose of preparing and sustaining polluted locations, with the aim of conserving aquifers that have been compromised due to both natural and human-induced factors. Hence, it is imperative to possess a comprehensive understanding of the intricate mechanisms governing groundwater chemistry in order to effectively comprehend and address the various concerns associated with this vital natural resource^{29,49,54}.

The Water Quality Index (WQI) provides a concise, single-number representation of water quality at different usage stages, covering physical, chemical, and biological characteristics. It effectively summarizes the overall condition of surface water^{51,52,61,63}. The WQI is calculated by combining several criteria into a single number, indicating water quality or pollution status. It helps predict contaminants, compare water quality from different sources, and guide water resource management^{16,47}. The task of computing the WQI becomes challenging due to the complexity and size of the data matrix, which encompasses several characteristics. In order to address this issue and mitigate subjectivity, several multivariate approaches like as Principal Component Analysis (PCA), component analysis, and others are used to provide a more comprehensive interpretation of the findings^{1,20}.

Therefore, this study aims to provide a baseline for evaluating water quality in the Southern Western Ghats, particularly in Kerala, India, with the following main objectives.

- Evaluated physico-chemical characteristics of groundwater samples and assessed hydrogeochemical processes using geochemical modeling, hydrochemical facies studies, and various graphical plots (Chadha diagrams, Gibbs plots, ion exchange reaction plots).
- Analyzed ion exchange, rock-water interaction, dissolution processes, and calculated saturation indices for selected minerals, correlating them with electrical conductivity.
- Applied statistical methods including PCA, correlation matrix with z-score standardization, and conducted Pearson correlation analysis to determine key factors influencing water quality, followed by calculating the water quality index

Methodology

Study Area

The study area encompasses part of the Western Ghats located within the state of Kerala, spanning across 11 out of the total 14 districts. The Western Ghats (hills) constitute a faulted escarpment that is mostly built out of the Deccan plateau and spans roughly 1600 kms parallel to the west coast of India from Gujarat to Tamil Nadu. The current study area extends 25,261 square kilometres and is situated between the boundaries of Tamil Nadu state to the east and the midland of Kerala. The area exhibits an average elevation of 900 m, featuring numerous peaks surpassing the altitude of 1800 m. This area gives rise to a total of 41 rivers that flow in a westward direction, while only three rivers flow in an eastward direction. The region experiences an average annual rainfall of 3060 mm, primarily occurring during the Southwest Monsoon season, which spans from May to September, followed by the Northeast Monsoon season, which takes place in November and December.

This region is characterized by the presence of significant plantations, including those dedicated to the cultivation of tea, coffee, rubber, and a variety of spices. This region is characterized by the presence of significant plantations, including those dedicated to the cultivation of tea, coffee, rubber, and various spices. This geographical region is commonly referred to as the Cardamom Hills. This particular geographical area is renowned for its significant contribution to the production of various spices, with a particular emphasis on cardamom, from which it derives its distinctive appellation. The highest peak in India after the Himalayas, Anaimudi (2694 m), is located in the Munnar region of the Western Ghats⁶⁴. In certain areas of their ranges, they are rich in mineral resources

such as iron, manganese, and bauxite ores. The practice of sand mining has become a significant concern in this region. The implementation of flawed cultivation practices, inadequate maintenance of drainage systems, and unsustainable mining activities have contributed to heightened susceptibility to landslides, compromised water sources, and impaired agricultural productivity.

The study area is situated within the Precambrian terrain of South India, characterized by the prevalence of charnockites and charnockitic gneisses as the dominant rock types (Fig. 1). The Western Ghats in Kerala are predominantly characterized by the presence of charnockitic gneisses and pyroxene-bearing granulites, particularly in the central and northern regions. These rocks cover around 40–50% of the entire area of the state. The prevalence of charnockites and their associated gneisses persists along the trends of the Western Ghats until reaching the Palaghat Gap. In addition to the mentioned above, the Palakkad and Idukki districts exhibit exposed rocks from the Peninsular Gneissic Complex, primarily consisting of hornblende-biotite gneisses and foliated granites. In the southern region, situated beyond the Palaghat Gap, the predominant rock formations consist primarily of khondalites accompanied by garnet-sillimanite-bearing gneisses. The state is characterized by the presence of extensive coastline, which is primarily composed of tertiary sedimentary deposits⁹.

Sampling and analysis

A total of 57 samples were included in this study, which were collected from the study area during the pre-monsoon season of 2021. For the collection of groundwater samples, two approaches were used: one for basic parameters, including hydrogen-ion-concentration (pH), electrical conductivity (EC), total dissolved solids (TDS), calcium (Ca^{2+}), magnesium (Mg^{2+}), sodium (Na^+), potassium (K^+), bicarbonate (HCO_3^-) chloride (Cl^-), sulphate (SO_4^{2-}), nitrate (NO_3^-), and fluoride (F^-), and another for metals such as iron and manganese following the standard chemical water quality procedures of American Public Health Association (APHA 2012). The groundwater samples were determined for the chemical parameters at Regional Chemical Laboratory, Central Ground Water Board, Kerala Region, Trivandrum, India. In order to perform basic parameter analysis, the groundwater samples were collected using one-liter HDPE bottles without acidification. While, for metals analysis, 100 mL polyethylene bottles were used. Samples were filtered using a mixed cellulose esters (MCE) membrane filter with a 0.45 μm pore size and acidified with ultrapure 65% nitric acid (0.5 mL per 100 mL of water) after filtration. This acidification step was performed to prevent any potential alterations in concentrations. Upon completion of the sample collection process, the samples were appropriately labeled, stored, and subsequently transported to the chemical laboratory for comprehensive chemical analysis.

For the analysis of the corresponding parameters, calibrated pH and EC meters were employed. The EC was used to calculate the TDS using the formula $\text{TDS (mg/L)} = \text{EC } (\mu\text{S/cm}) \times 0.64$, as suggested by Elumalai¹⁵. The procedures for analysis were implemented by the American Public Health Association⁴. Analyses of bicarbonate were conducted using an acid titration method with phenolphthalein and methyl orange as indicators. The Ion Chromatography instruments (Metrohm 930) were used to analyse the anions and cations³⁰. To ensure the accuracy and precision of the analysis, standards and blanks were run repeatedly. Analytical precision and measurement reproducibility were under 2%, whereas the ionic balance error for analyzed ions was $\pm 5\%$. The

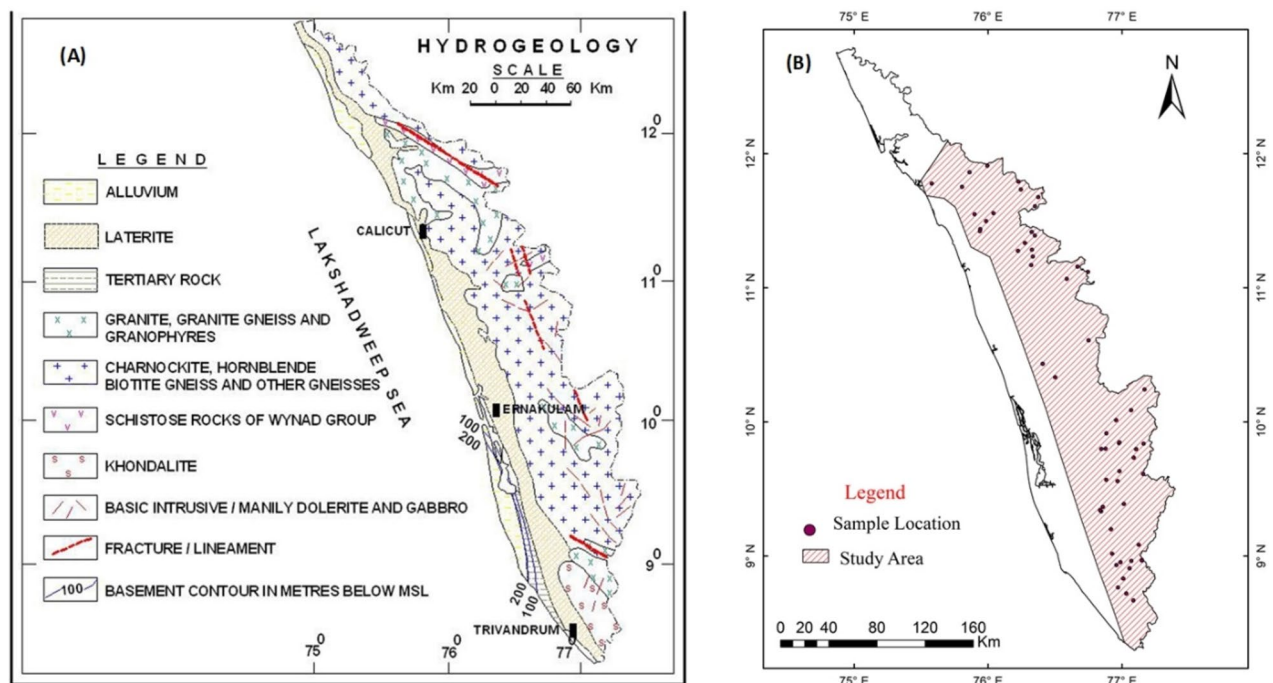


Figure 1. Study area. (A) Hydrogeological characteristics (B) Sample locations. This map was generated using ESRI's ArcGIS 10.7 for Desktop software (<http://www.esri.com>), version 10.7.1.

Atomic absorption spectrophotometer -Flame was used to analyze heavy metals (PerkinElmer 800, Waltham, Massachusetts, USA). The detection limits for the metals Fe and Mn were 0.05 and 0.02 mg/L, respectively. The standard solution was made from a 1000 mg/L stock solution of metals of interest to obtain the metal ion calibration curve. Laboratory quality control and quality assurance measures, including standard operating procedures, standard calibration, and reagent blank analysis, were used to ensure the accuracy of the analytical results.

Water quality index

The WQI is a grading technique that evaluates the collective impact of various water quality parameters on the overall suitability of water for human consumption. It is often used to describe the availability and suitability of potable water resources for domestic use. There are numerous water indices developed by national and international organizations, such as the Weight Arithmetic Water Quality Index (WAWQI), the National Sanitation Foundation Water Quality Index (NSFWQI), the Canadian Council of Ministers of the Environment Water Quality Index (CCMEWQI), and the Oregon Water indices, which are employed worldwide.

The current research used the Weight Arithmetic Water Quality Index methodology as outlined by Subba Rao⁵⁷. The calculation included the values of 13 parameters that were analyzed in a total of 57 samples. The computation of Water Quality Index included a series of five steps. The first step included the assignment of unit weight (U_w) to each chemical parameter (i), based on its relative significance in relation to human health. In this particular case, 5 were given to the parameter with the highest significance and 1 to the parameter with the lowest significance (Table 1). The calculation of the relative weight (R_w) for each chemical parameter was performed in the second step, as described by Eq. (1). The percentage of quality rating scale (Q_R) was calculated in the third step by dividing the concentration of chemical parameter (C) by its standard drinking water quality (D) for each chemical parameter (Eq. 2). In the fourth step, the determination of the relative rating (R_R) was computed by multiplying the relative weight (R_w) with the quality rating (Q_R) for each chemical parameter, as seen in Eq. (3). Finally, the WQI was calculated by summing all R_R in each sample (Eq. 4).

$$R_w = \frac{U_w}{\sum_{i=1}^n U_w} \quad (1)$$

$$Q_R = \frac{C}{D} \times 100 \quad (2)$$

$$R_R = R_w \times Q_R \quad (3)$$

$$WQI = \sum R_R \quad (4)$$

Saturation indices

Saturation indices are calculated using the equation $SI = \log(IAP/K_s)$, where IAP and K_s are the ion activity and solubility products, respectively. If $SI = 0$, the corresponding mineral is in equilibrium in the aquifer, whereas $SI > 0$ and $SI < 0$ indicate oversaturation and undersaturation of the mineral in the water, respectively. This approach has been employed in other studies to investigate how mineral weathering affects the chemistry of water^{32,69}

Multivariate statistical methods

The Multivariate statistical analysis approach was used to identify geochemical processes, dissolved constituent sources, and their origins. Pearson correlation analysis and hierarchical cluster analysis were performed using

Chemical parameters	D	U_w	R_w	References
pH	8.5	4	0.08	BIS (2012)
TDS (mg/L)	500	5	0.1	BIS (2012)
Ca ²⁺ (mg/L)	75	2	0.04	BIS (2012)
Mg ²⁺ (mg/L)	30	2	0.04	BIS (2012)
Na ⁺ (mg/L)	200	4	0.08	BIS (2012)
HCO ₃ ⁻ (mg/L)	300	1	0.02	BIS (2012)
Cl ⁻ (mg/L)	250	5	0.1	BIS (2012)
SO ₄ ²⁻ (mg/L)	200	5	0.1	BIS (2012)
NO ₃ ⁻ (mg/L)	45	5	0.1	BIS (2012)
F ⁻ (mg/L)	1.5	5	0.1	BIS (2012)
K ⁺ (mg/L)	12	2	0.04	Subba Rao et al. (2019)
Fe (mg/L)	0.3	5	0.1	BIS (2012)
Mn (mg/L)	0.1	5	0.1	BIS (2012)

Table 1. Particulars of desirable limits (D), unit weight (U_w) and relative weight (R_w) for WQI.

Origin Pro 2022 (OriginLab), while IBM Statistical Package of Social Studies (SPSS) version 26 software was used for the factor analysis, which was computed with the help of the principal component analysis extraction method. PCA analysis was performed using Varimax rotation with Kaiser Normalization. The analysis considered eigenvalues greater than one and extracted three main components. These three components were plotted in a three-dimensional box to facilitate a better understanding of geochemical data. To group the sampling locations with similar hydrogeochemical behavior, a hierarchical cluster analysis was carried out in the form of a polar heat map, which was performed using the squared Euclidean distance and Ward's technique. To eliminate bias and the effects of individual factors, the water quality data set was standardized and converted into a z-score prior to carrying out the PCA and HCA analyses^{14,45}. The correlation between variables was estimated using Pearson's correlation coefficient (*r*). Microsoft Excel 2016 was used throughout the process of both the descriptive statistics and the data management.

Results and discussion

The results of descriptive statistical analysis on the quality data are shown in Fig. 2. The pH of the groundwater ranged from 3.06 to 8.35, with an average value of 7.08, suggesting that it is acidic to alkaline in nature (SI Table 1. Statistics for analysed parameter). Groundwater samples may be categorized as acidic (pH < 6.5, 12%, N = 7), neutral (pH 6.5–7.5, 44%, N = 25), or alkaline (pH > 7.5, 44%, N = 25). Groundwater samples with high acidic pH include S6 (3.06), S16 (4.40), S43 (4.00), S47 (4.10), and S48 (3.60). The lower pH might be attributed to the high rain fall and low water table condition, which favors slightly acidic water in shallow aquifer systems, especially lateritic terrains like the samples above^{12,13,22,24}. The EC ranged from 50 to 970 $\mu\text{S}/\text{cm}$, with an average of 266 $\mu\text{S}/\text{cm}$. EC < 250 $\mu\text{S}/\text{cm}$ is found in around 67% of the samples (N = 38). TDS was determined from EC using the formula $\text{TDS (mg/L)} = \text{EC (}\mu\text{S/cm)} \times 0.64$, and the average value ranged from 32 to 621 mg/l. Results showed that the TDS levels were found to be < 100 mg/l in 26 samples (46%) and < 250 mg/l in 46 samples (81%). The low TDS is a result of the high rainfall received here during the monsoon season. Because of this intense rainfall and steep topographic gradient actively flushes the products of weathering leading to low dissolved solids in ground water. According to WHO⁶⁶, the results of the total hardness (TH) classification show that there are different classes of groundwater in the study area, including soft groundwater (TH < 60 mg/l, N = 34), moderately hard groundwater (60 > TH < 120 mg/l, N = 13), hard groundwater (120 > TH < 180 mg/l, N = 5), and very hard groundwater (TH > 180 mg/l, N = 5).

EC, TDS, and TH have corresponding standard deviations of 231 $\mu\text{S}/\text{cm}$, 148 mg/l, and 69 mg/l. The descriptive statistical analysis of the major cations and anions are shown in SI Table 1. The standard deviation is an excellent tool for determining groundwater features in any location^{15,60,70}. High standard deviations in TDS, EC,

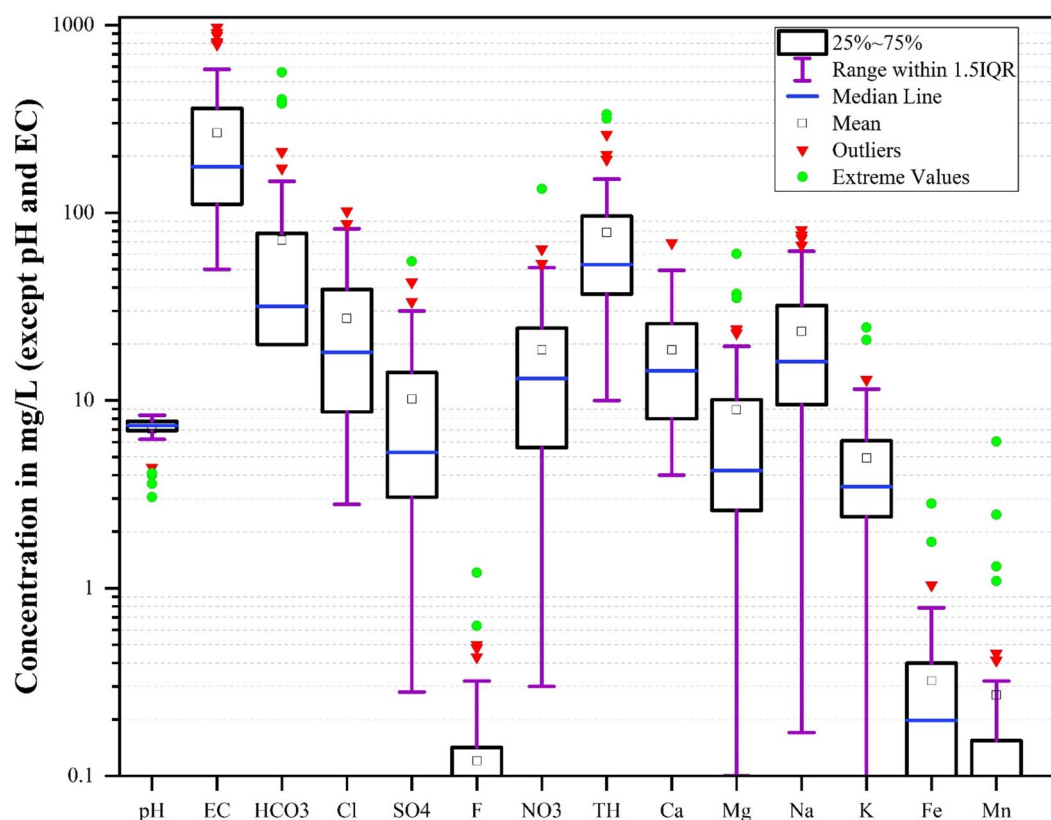


Figure 2. Box pot showing the chemical composition of groundwater in study area.

and TH were reported in this research, indicating that the sources of chemical components in this aquifer come from diverse geochemical processes.

High enrichments of Fe and Mn are reported in this study area. The Fe ranges between <0.05 mg/l and 2.83 mg/l, with an average of 0.32 mg/l. (Fig. 2). The samples with $N=19$ show $Fe > 0.3$ mg/L, which is above the acceptable limit as prescribed by BIS⁷, for drinking purpose, while the samples with $N=37$ show $0.1 > Fe < 0.3$ mg/l. Similarly, the Mn ranges between <0.02 mg/l and 6.05 mg/l, with a mean of 0.27 mg/l. (Fig. 2). The samples with $N=16$ show $Mn > 0.1$ mg/L, which is beyond the acceptable limit as recommended by BIS for drinking purpose, whereas the samples with $N=9$ show $0.05 > Mn < 0.1$ mg/l.

Water quality index (WQI)

Based on the WQI^{20,31,35}, groundwater quality is graded as follows: excellent quality (<25), good quality (25–50), average quality (51–75), poor quality (76–100), and unsuitable quality (>100). The computed values of the WQI in the present study area is ranged from 14 to 621 in the groundwater samples, with an average value of 60. Among these samples, 42% ($N=24$) were classified as having good quality (WQI 26–50), while 26% ($N=15$) were categorized as having excellent quality (WQI <25). Furthermore 19% ($N=11$) were categorized as having average quality (WQI 51–75). Interestingly, only a small share of the samples, specifically 5% ($N=3$), fell into the Poor Quality category (WQI 76–100). These findings highlight the overall favourable water quality conditions observed in the samples analysed. It is worth noting that only a small proportion of the samples, specifically 7% ($N=4$), were classified as belonging to the category of unsuitable quality, as indicated by a WQI >100 . Thus, the aforementioned results underscore the overall good water quality characteristics seen in the studied samples.

Using the spatial distribution of WQI as depicted in Fig. 3A, it is possible to evaluate the variation of WQI classes throughout the study area. About half of the study area, including 12,735 square kilometres, is classified as Excellent to Good Quality and this classification encompasses mainly Kollam, Kozhikode, Kannur and Wayanad districts. About 39% (9,971 sq. km) and 3% (885 sq. km) of the total area fell into the categories of Average Quality and Poor Quality, respectively, with the majority of these areas located in the districts of Palakkad, Kottayam, Thiruvananthapuram and Idukki. Subsequently, the unsuitable drinking water quality category encompasses about 8% (1953 sq. km) of the overall study area, mostly concentrated in the south part of Idukki district and a north portion of Pattanamtitta district. Additionally, south eastern part of Wayanad district also fall in this category. The high WQI value in this region is due to excessive concentration of Fe and Mn in the groundwater, which primarily derives from the geogenic source (Fig. 3B, C).

Hydrochemical facies

Lithospheric composition, groundwater movement, and other natural activities all affect the hydrochemical facies in the groundwater. In this study area, ions that prevail in groundwater are $Na^+ > Ca^{2+} > Mg^{2+} > K^+$ and $HCO_3^- > Cl^- > NO_3^- > SO_4^{2-}$. The Chadha diagram¹⁰ (Fig. 4D) are used to investigate the hydrochemical facies of the study region. The Chadha diagram reveals that the groundwater samples were scattered across three major zones, with the exception of four samples. The samples have been clustered together as follows: $CaHCO_3$ facies (46%) $>$ $CaMgCl$ facies (30%) $>$ $NaCl$ facies (17%) $>$ $NaHCO_3$ facies (7%). The facies of $NaCl$ and $CaMgCl$ of groundwater show the effect of ion exchange processes, evaporation, and prolonged storage/residence but the mineral weathering process is only expected to have an impact on groundwater with $CaHCO_3$ facies^{14,45}. The $CaHCO_3$ facies is observed in the majority of the samples from the district of Wayand, Pathanamthitta, Palakkad and Thrissur, and it exhibits the Recharging water features. Furthermore, $CaMgCl$ facies indicate the reverse ion exchange properties of water, as found in the majority of samples from districts of Kazikhode, Malappuram, and

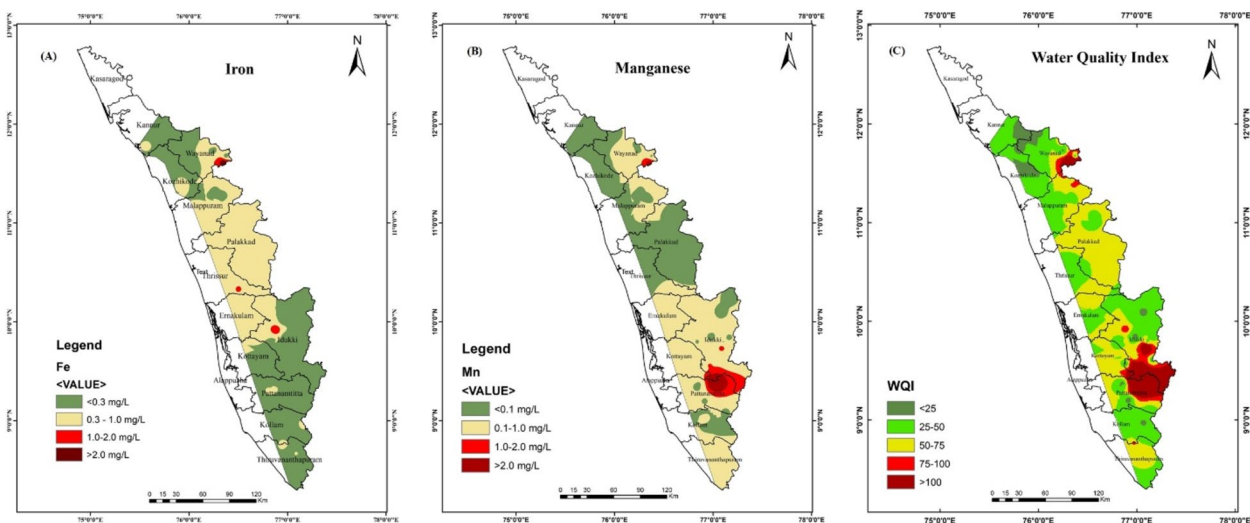


Figure 3. Spatial distribution of Iron (A), Manganese (B), and Water Quality Index (C) in study area. This map was generated using ESRI's ArcGIS 10.7 for Desktop software (<http://www.esri.com>), version 10.7.1.

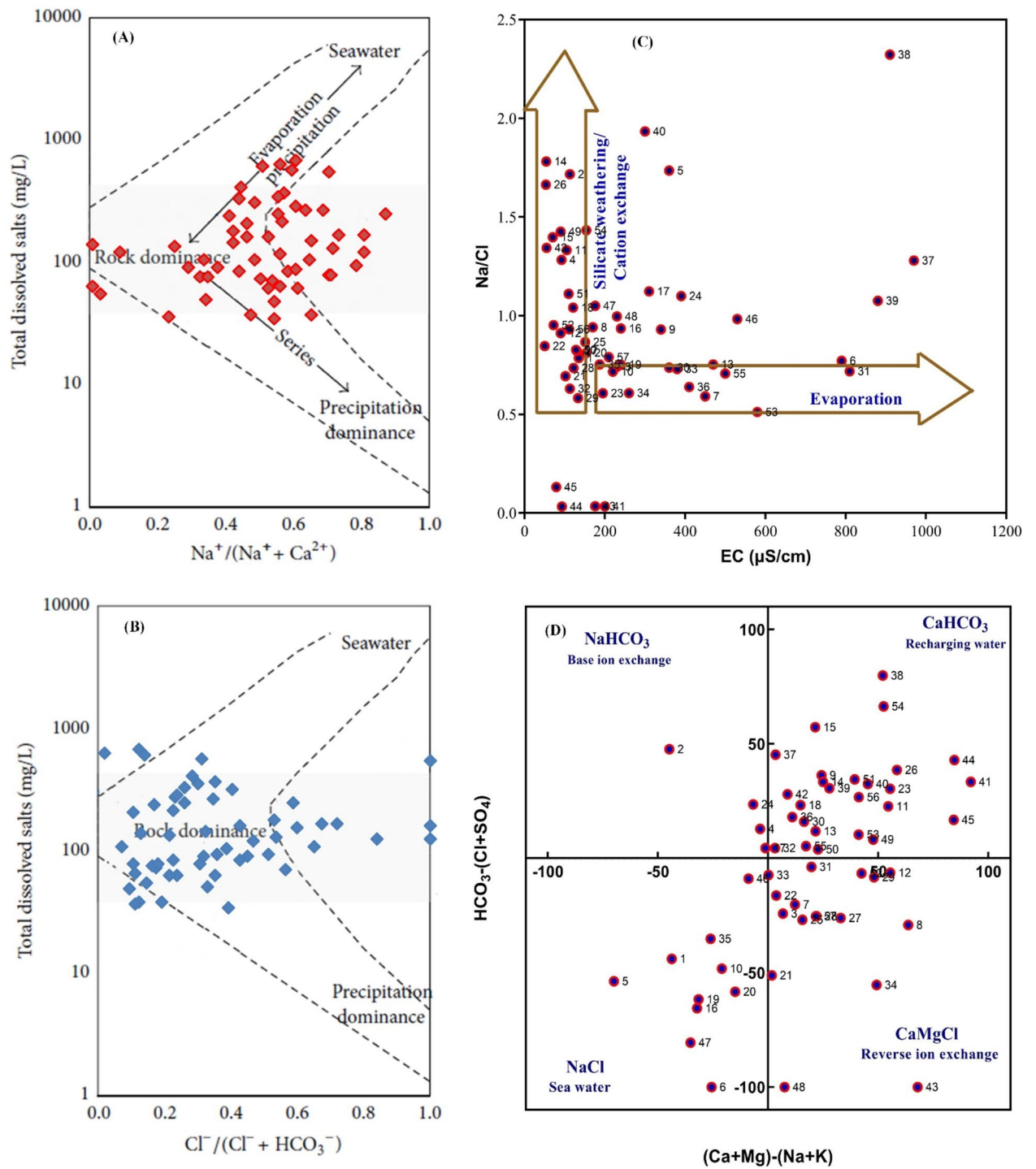


Figure 4. Factors influencing the chemistry groundwater chemistry. (A) Gibbs plot for cation, (B) Gibbs plot for anion, (C) Relation between Na/Cl and EC, (D) Chadha diagram.

Kottayam. However, the NaCl facies is only seen in the majority of Trivandrum district samples. This facies represents salt water as a result of a high EC. Subsequently, only four samples, two from the Idukki district and two from the Kollam district, exhibit NaHCO₃ facies, which is indicative of the base ion exchange properties of the water. The samples from the districts of Idukki and Kollam display mixed hydrochemical facies with an asymmetrical trend. SI Table 2 (Hydrochemical facies distribution) displays the hydrochemical facies distribution across district.

Influencing hydrogeochemical processes

To distinguish the influential hydrogeochemical processes in this aquifer, Gibbs and bivariate plots were used.

Gibbs plots

Gibbs employed the TDS and ionic ratios as a means of discerning the primary geochemical mechanisms that govern the chemical composition of water. In the cation plot and the anion plot (Fig. 4A, B), the TDS is plotted against the $\text{Na}^+ + \text{K}^+/\text{Na}^+ + \text{K}^+ + \text{Ca}^{2+}$ ratio and against the $\text{Cl}^-/\text{Cl}^- + \text{HCO}_3^-$ ratio, respectively. Evaporation, mineral weathering, and rainfall input may all be readily distinguished using these graphs. Ca^{2+} and HCO_3^- will be removed from the system during the process of evaporation by carbonate precipitation, which will then be followed by TDS enrichment in the aquifer⁴⁵. As a result, the concentrations of Na^+ and Cl^- in groundwater will rise. In the current study, around 10% of the samples are fall in precipitation zone and rest of the samples cluster in a zone of mineral weathering. No samples are depicted on the evaporation zone. Mineral weathering is the dominant process followed by precipitation in the area of study.

Evaporation

As reported by Jankowski and Acworth²³, the plot of EC against Na^+/Cl^- will not change with increasing salinity (EC) if evaporation is the dominating process in water chemistry. When Na^+/Cl^- is plotted against EC, as shown in Fig. 4C, only a few wells follow the trend of evaporation. This demonstrates that evaporation is not the dominant factor that influences the chemistry of water⁴⁴. Figure 4C shows that the Na^+/Cl^- ratios are enriched and depleted, indicating that silicate dissolution and the ion exchange mechanism are primarily controlling the water chemistry^{36,44}.

Carbonate dissolution on water chemistry

Ionic ratios and bivariate plots are used in order to evaluate the influence of carbonate dissolution on chemistry water. Results of carbonate mineral dissolution in the groundwater yield of Ca^{2+} , Mg^{2+} , and HCO_3^- ^{33,44,46}. In this study, the average $\text{Ca}^{2+}/\text{Mg}^{2+}$ molar ratio is 2.6, which varied from 0.19 to 9.7 (one sample is eliminated because of its exceptional value of 24.5), and it is greater than 1 in 74% of the samples (Fig. 5). About 40% of the samples have a $\text{Ca}^{2+}/\text{Mg}^{2+}$ ratio greater than 2. According to Maya and Loucks³³, dolomite dissolution will retain a ratio of 1, whereas calcite dissolution will result in a ratio greater than 1. The higher ratio of $\text{Ca}^{2+}/\text{Mg}^{2+}$ (>2) is due to silicate weathering in the system^{43,46}. In the present study area, water samples that are close to $\text{Ca}^{2+}/\text{Mg}^{2+}$ the = 1 line indicates that dolomite dissolution, while clusters that are between 1 and 2 reveal that the dissolution of calcite. The existence of an impact from silicate weathering in this aquifer is indicated by higher ratios, ($\text{Ca}^{2+}/\text{Mg}^{2+} > 2$).

Silicate weathering

As previously stated, silicate weathering influenced the major ion chemistry in this aquifer⁴³. Furthermore, the Na^+/Cl^- ratio in this aquifer ranges from 0.05 to 3.58, with an average of 1.45 (Fig. 5). The dissolution of halite will maintain a 1:1 Na^+/Cl^- ratio. However, the weathering of silicates and cation exchange resulted in a rise in the system's sodium content, which led to a ratio of sodium to chloride greater than one. In this study area, around 81% of samples indicate a higher ratio ($\text{Na}^+/\text{Cl}^- > 1$), and the sodium content in these wells is obtained through silicate weathering and cation exchange. In order to confirm the impact of mineral weathering and ion exchange reaction, the relationship between $\text{Ca}^{2+} + \text{Mg}^{2+}$ and $\text{HCO}_3^- + \text{SO}_4^{2-}$ is exercised. If the Ca^{2+} and Mg^{2+} resulted as a consequence of the weathering of carbonate, sulphate (gypsum, anhydrite), and silicate minerals, then the $\text{HCO}_3^- + \text{SO}_4^{2-}$ will balance both of those elements^{8,34}. The water samples plotted on or near the 1:1 line in Fig. 5B illustrate the influence of mineral weathering on water chemistry in the current study. However, samples plotted above or below the equiline indicate the existence of alternative processes. Similarly, to investigate and distinguish the effects of weathering of silicates, carbonates, and evaporites/evaporation in the aquifer, molar $\text{Ca}^{2+}/\text{Na}^+$ is plotted versus molar $\text{HCO}_3^-/\text{Na}^+$ ^{18,46}. The samples were distributed in a cluster between the evaporation zone and the silicate weathering zone, as shown in Fig. 5. These elements are mostly derived through silicate weathering. The precipitation of carbonate minerals and the subsequent increase in Na^+ concentration in the aquifers are explained by samples plotted on or near the evaporation zone. As a result of the weathering of soda feldspar (albite), potash feldspar, orthoclase, and microcline, Na^+ and K^+ ions are released into the aquifer^{15,39}.

Ion exchange reactions

Cation exchange or silicate weathering are accountable for the enriching of Na^+ over Cl^- , while reverse ion exchange events are accountable for the depleting of Na^+ over Cl^- . The ion exchange process is further confirmed by the plot of $\text{Ca}^{2+} + \text{Mg}^{2+}$ vs $\text{HCO}_3^- + \text{SO}_4^{2-}$ in Fig. 5B. The presence of a high $\text{Ca}^{2+} + \text{Mg}^{2+}$ concentration over $\text{HCO}_3^- + \text{SO}_4^{2-}$ in about 20% of the samples suggests a reverse ion exchange process. $\text{Ca}^{2+} + \text{Mg}^{2+}$ depletion over $\text{HCO}_3^- + \text{SO}_4^{2-}$ confirms that $\text{Ca}^{2+} + \text{Mg}^{2+}$ is withdrawn from groundwater by cation exchange reaction or Na^+/K^+ silicates weathering should have increased HCO_3^- ⁴⁵. Similarly, the ratio of $\text{Na}^+ + \text{K}^+$ to HCO_3^- demonstrates an elevation of $\text{Na}^+ + \text{K}^+$ in relation to HCO_3^- as a result of cation exchange activities (Fig. 5D). Schoellar, described the chloroalkaline indices (CAI 1 and CAI 2), which were used in several studies to elucidate ion exchange processes in groundwater⁵⁰.

The negative values of CAI 1 and CAI 2 indicate cation exchange process whereas positive values indicate reverse ion exchange. High concentrations of $\text{Na}^+ + \text{K}^+$ over Cl^- result in negative values in these calculations, indicating cation exchange processes, whereas high concentrations of Cl^- over $\text{Na}^+ + \text{K}^+$ result in positive values, indicating reverse ion exchange reactions. The majority of the samples (91%) had negative values and show a negative trend, as seen in Fig. 5E. Therefore, cation exchange reaction plays a crucial role in controlling water chemistry, whereas only five samples exhibit positive values indicative of reverse ion exchange reaction. In the case of a cation exchange reaction, the plot of $\text{Ca}^{2+} + \text{Mg}^{2+} - \text{Alk} - \text{SO}_4^{2-}$ versus $\text{Na}^+ + \text{K}^+ - \text{Cl}^-$ will exhibit a negative slope and a significant negative correlation. Figure 5F depicts a negative slope with a significant negative

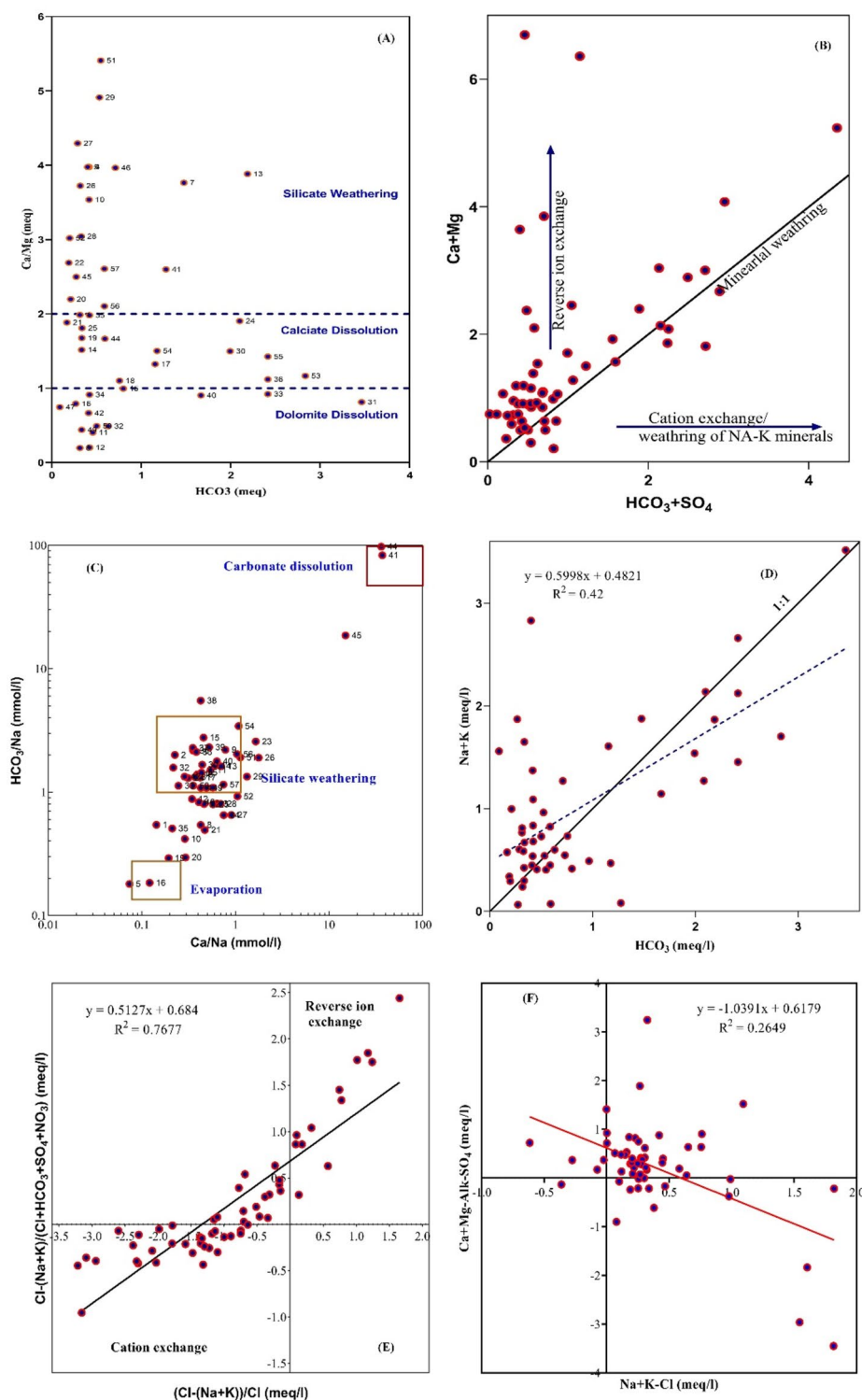


Figure 5. Influence of mineral weathering and ion exchange processes on groundwater chemistry. (A) Plot of HCO_3^- Vs $\text{Ca}^{2+}/\text{Mg}^{2+}$ for Carbonate dissolution, (B) Plot of $\text{HCO}_3^- + \text{SO}_4^{2-}$ Vs Na^+/Cl^- for Silicate weathering, (C) Plot of $\text{Ca}^{2+}/\text{Na}^+$ Vs $\text{HCO}_3^-/\text{Na}^+$ for distinguish the effects of weathering, (D) Plot of HCO_3^- Vs $\text{Na}^+ + \text{K}^+$ for elucidation of ion exchange processes, (E) Plot of Cl^- over $\text{Na}^+ + \text{K}^+$ for elucidation of hydrochemical process, (F) Plot of $\text{Na}^+ + \text{K}^+ - \text{Cl}^-$ Vs $\text{Ca}^{2+} + \text{Mg}^{2+} - \text{Alk} - \text{SO}_4^{2-}$ for weathering and ion exchange processes.

correlation, proving that cation exchange reactions in addition to mineral weathering influence the water chemistry in the study area.

Geochemical modelling

Commonly, aqueous geochemical calculations are often used to examine the interactions between rocks and minerals employing a thermodynamic database. The identification of silicate weathering and carbonate mineral dissolution is facilitated by these calculations¹¹. Based on available data, the PHREEQC algorithm was used to determine the ionic strength and saturation indices for selected minerals^{40,41}. Ionic strength in the current study ranged from 0.0009 to 0.014, with an average value of 0.004. The ionic strength has a significant correlation with EC as seen in Fig. 6. Further, the average value of the partial pressure of CO₂ (pCO₂) was found to be 2.88, and it

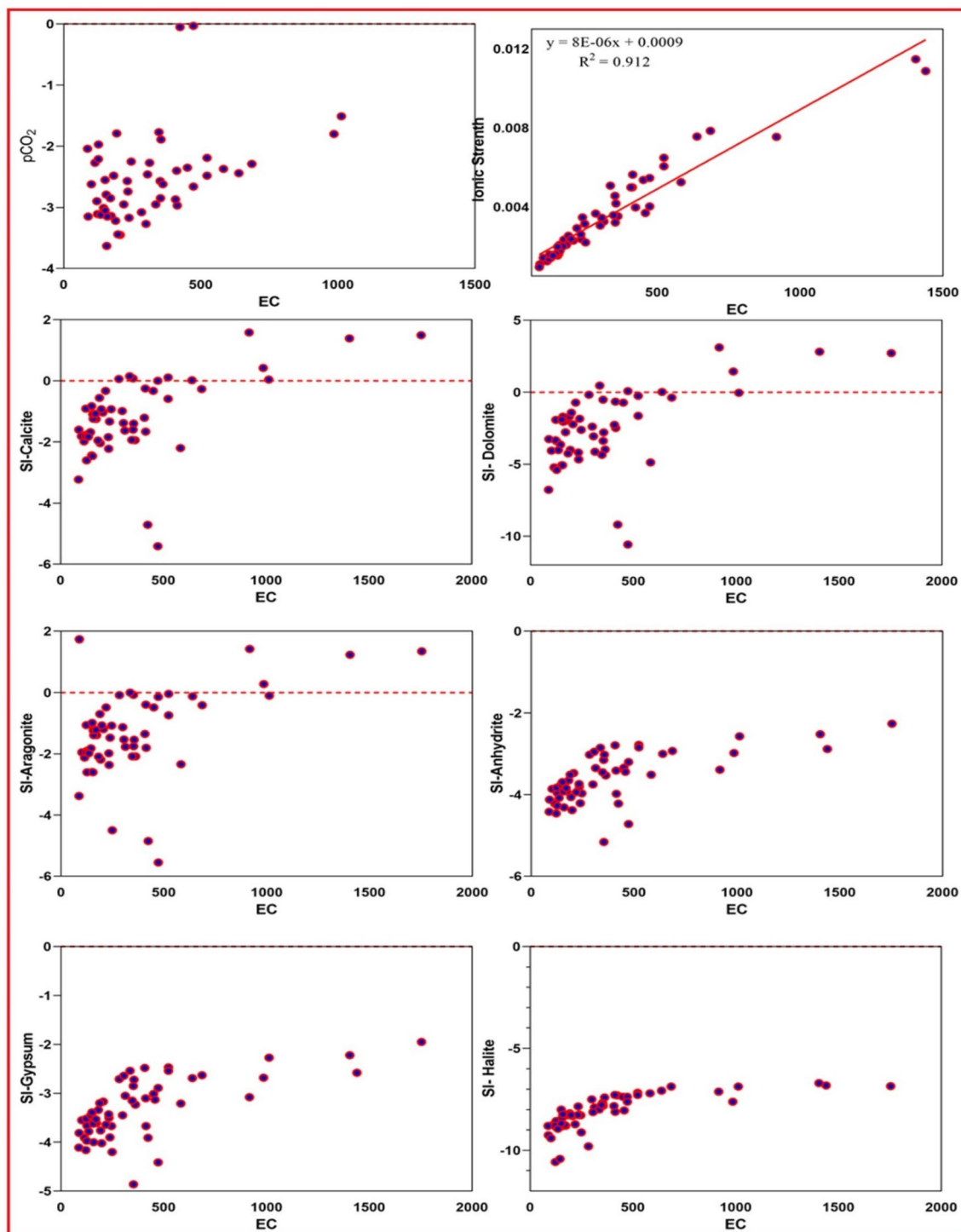


Figure 6. Saturation indices of carbonate minerals and their relation with salinity in the groundwater.

ranged from -9.24 to 0.03 . At the location of the study, the $p\text{CO}_2$ levels in the water samples are mainly greater than the atmospheric $p\text{CO}_2$ (-3.4), with the exception of six wells. Wells with more salinity water have $p\text{CO}_2$ higher values, which are strongly associated with the atmosphere, and the relationship between EC and $p\text{CO}_2$ also shows a positive tendency (Fig. 6). The $p\text{CO}_2$ numbers may be related to the groundwater level, and deep wells tend to have low EC and $p\text{CO}_2$. However, groundwater level data is not used to conform this information for sampling wells.

According to SI calculations and Fig. 6, about 20% of groundwater sample wells are saturated with carbonate minerals such as calcite (CaCO_3), aragonite (CaCO_3), dolomite ($\text{CaMg}(\text{CO}_3)_2$), siderite (FeCO_3), and rhodochrosite (MnCO_3), indicating that dissolution of carbonate minerals regulates groundwater chemistry. The fact that the groundwater has high concentrations of Ca^{2+} , Mg^{2+} , and HCO_3^- , as well as a neutral to alkaline pH, is further evidence that carbonate reactions are crucial for preserving the hydrochemistry of the groundwater in multilevel wells. The dolomite saturation index values range widely across the sample wells (-10.5 to 3.1). The existence of carbonate minerals and their wide variation are crucial because ground level variations in the sample wells may have caused calcite and aragonite to dolomitize as a result of an interaction with groundwater that contains magnesium.

Groundwater tends to be supersaturated with hematite (Fe_2O_3), goethite (FeOOH), and ferrihydrite ($\text{Fe}(\text{OH})_3$), as shown in Fig. 7. This indicates that there is a suitable thermodynamic environment for the precipitation of Fe(III) phases from groundwater. Meanwhile, when Fe(II) and Mn(II) concentrations increase, correspondingly increases the SI of siderite and rhodochrosite. Fe(II) and Mn(II) concentrations in groundwater are constrained by adsorption onto or co-precipitation with CaCO_3 , according to the saturation of groundwater with calcite, siderite, and rhodochrosite⁵. CaCO_3 may be partially substituted with Mn, which can lead to the creation of rhodochrosite^{37,65}. Therefore, these minerals have the ability to act as a sink by removing Fe(II) and Mn(II) ions from anoxic groundwater that contains a high concentration of HCO_3^- . Such processes can accelerate the rate at which Fe and Mn oxyhydroxide are reduced by shifting the equilibrium of redox towards the reduced phases of Fe (II) and Mn (II), respectively.

Multivariate statistical analysis

Pearson correlation analysis

Pearson correlation analysis was performed in this study and results are presented in Fig. 8A. Variables namely pH, Fe and Mn does not correlate with other variables. Additionally, pH shows significant negative correlation with NO_3^- and K^+ . EC and TH express strong positive correlation with all variables except NO_3^- , K^+ and pH. NO_3^- shows the significant correlation with only Na^+ , K^+ and Cl^- and rest of the parameter are not correlated with it whereas K^+ shows correlation with only NO_3^- . The positive correlation between NO_3^- and K^+ ($r^2 > 0.59$) suggest that both are derived from anthropogenic sources in this aquifer. Sulphate and chloride minerals are highly undersaturated in this aquifer. Therefore, Cl^- and SO_4^{2-} are good indicator of anthropogenic input. Variables correlated with Cl^- and SO_4^{2-} are partially or completely derived from anthropogenic sources. Similarly, with the exception of pH, K^+ , and NO_3^- , HCO_3^- has a substantial positive correlation with all variables. Also, none of the relationships between the concentration of metals (Fe and Mn) in water samples were significant. This means that the Fe and Mn in the water samples were not related to other parameter of water and may have come from different sources in the study area.

Principal component analysis (PCA)

One effective approach for identifying the origins of variables and geochemical processes is the PCA analysis. In PCA, the water analysis data is reduced and simplified into components. Tables 2 and 3 depicts the number of obtained factors with Eigen values greater than one, as well as variance and cumulative variance. Similarly, a graphical illustration is shown in Fig. 8B. In the current study, three factors account for about 77.1% of the variance. Factor 1 has a substantial positive loading on EC, TH, Na^+ , Mg^{2+} , Cl^- , HCO_3^- , and SO_4^{2-} , and it accounts for 50.2% of the variance. The main source of chemical constituents in this aquifer is mineral weathering which to some extent includes gypsum and halite for the contributing Cl^- and SO_4^{2-} in the aquifer. Therefore, elevated HCO_3^- loading implies those processes. Therefore, factor 1 validates the impact of geogenic processes. Factor 2 accounts for 17.9% of total variance and has a high positive loading of K^+ and NO_3^- . This factor illustrates the anthropogenic NO_3^- inflow into this aquifer. There is no correlation between NO_3^- and Cl^- , SO_4^{2-} , or other variables. Consequently, nitrification is the most probable source of NO_3^- in this aquifer. The application of fertilizers and manures in agricultural practices results in an increased presence of NO_3^- in groundwater due to infiltration in the vadose zone. Factor 3, which accounts for 9.0% of the total variance, exhibits positive loadings only for Fe and Mn. This indicates that the lack of correlation between Fe and Mn and other water characteristics suggests that their presence may be due to the weathering of local geological formations rich in these minerals, such as Laterite and Archaeans.

Hierarchical cluster analysis (HCA)

The results of HCA presented in the form of polar heat-map (Fig. 8C) with vertical dendrogram (Q-mode) represent the cluster of water parameters and horizontal dendrogram (R-mode) represent the cluster of sample location. There are four groups shown in Q-mode. Group 1 is associated with the elements EC, TH, Na^+ , Mg^{2+} , Cl^- , HCO_3^- , and SO_4^{2-} , which suggests that silicate and carbonate weathering, as well as gypsum and halite, are present to a certain extent. Group 2 consists of two variables, including NO_3^- and K^+ , and these variables indicate anthropogenic origins. Only pH exists in Group 3, and it is not affected by weathering or anthropogenic factors. Group 4 includes metals like Fe and Mn, which may indicate a potential independent origin such as the weathering of Laterite and Archaeans. Furthermore, in R-mode, there are three clusters with 75% samples ($n = 43$) fall

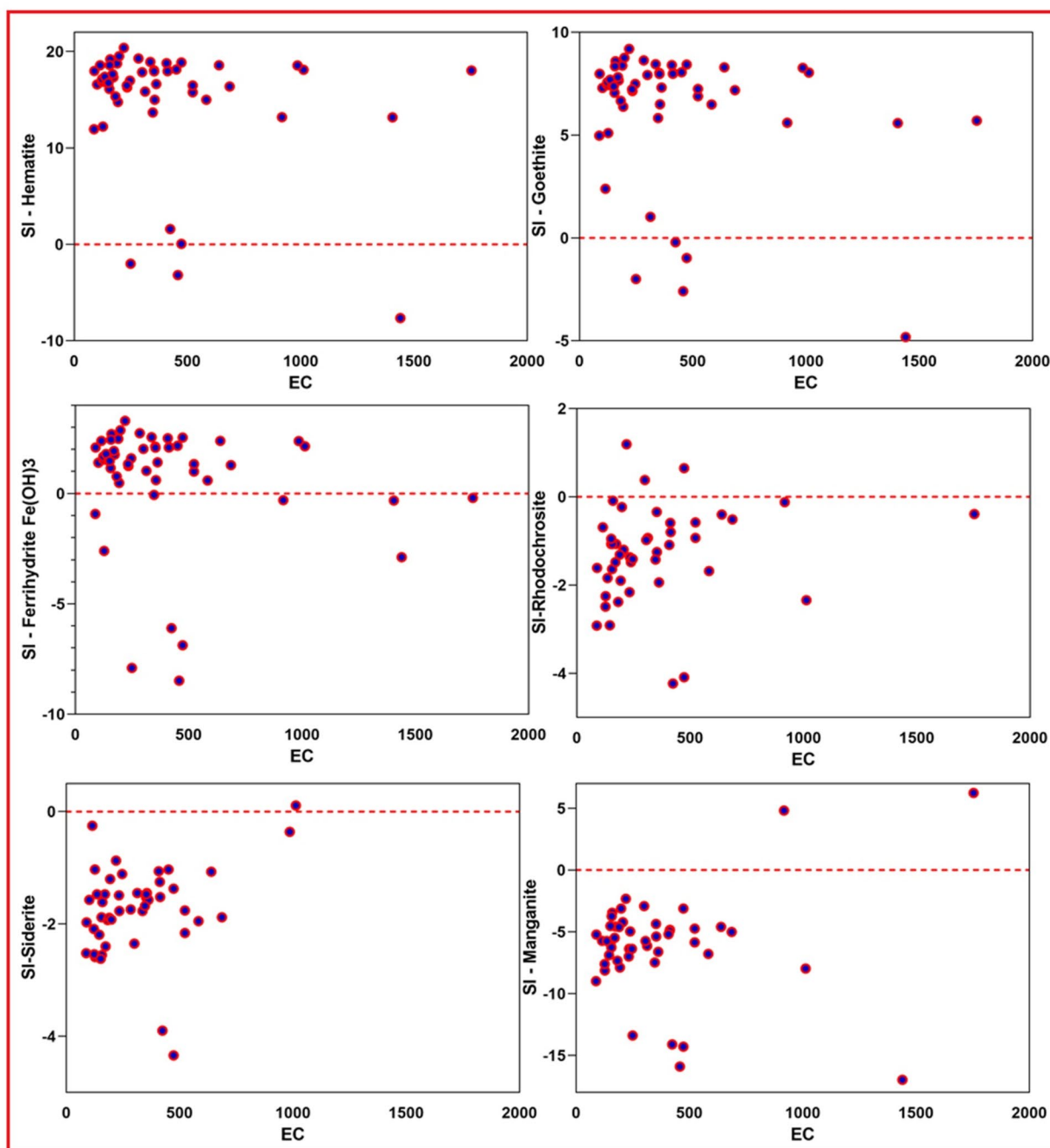


Figure 7. Saturation indices of Iron minerals and their relation with salinity in the groundwater.

under cluster 1, which is less mineralized, and the EC values with an average of 160 $\mu\text{S}/\text{cm}$ which suggest that groundwater is located nearby the aquifer recharge area. Cluster 2 accommodates 17% ($n=10$) samples with an average of 470 $\mu\text{S}/\text{cm}$. This cluster indicates that waters that were recharged relatively long ago and have flown a certain distance within the aquifer are moderately mineralized. The locations included in this cluster are mainly from Malappuram district and some parts of Idukki district. Only 4 samples (3 from Palakkad district and 1 from Malappuram district) are grouped in cluster 3. Groundwater in these wells is highly mineralized and EC, with an average value of 900, indicating high mineralization.

Conclusion

The study in the Western Ghats of the Kerala region utilized a multifaceted approach to unravel the complexities of groundwater chemistry. Results indicate groundwater has a pH range of neutral to alkaline with a acidic in certain samples, with EC and TDS below 1000 $\mu\text{S}/\text{cm}$ and 700 mg/l, respectively, for all samples, and it is classified as soft to very hard. This area has high Fe and Mn enrichments. The samples with 33 and 28% exceed the

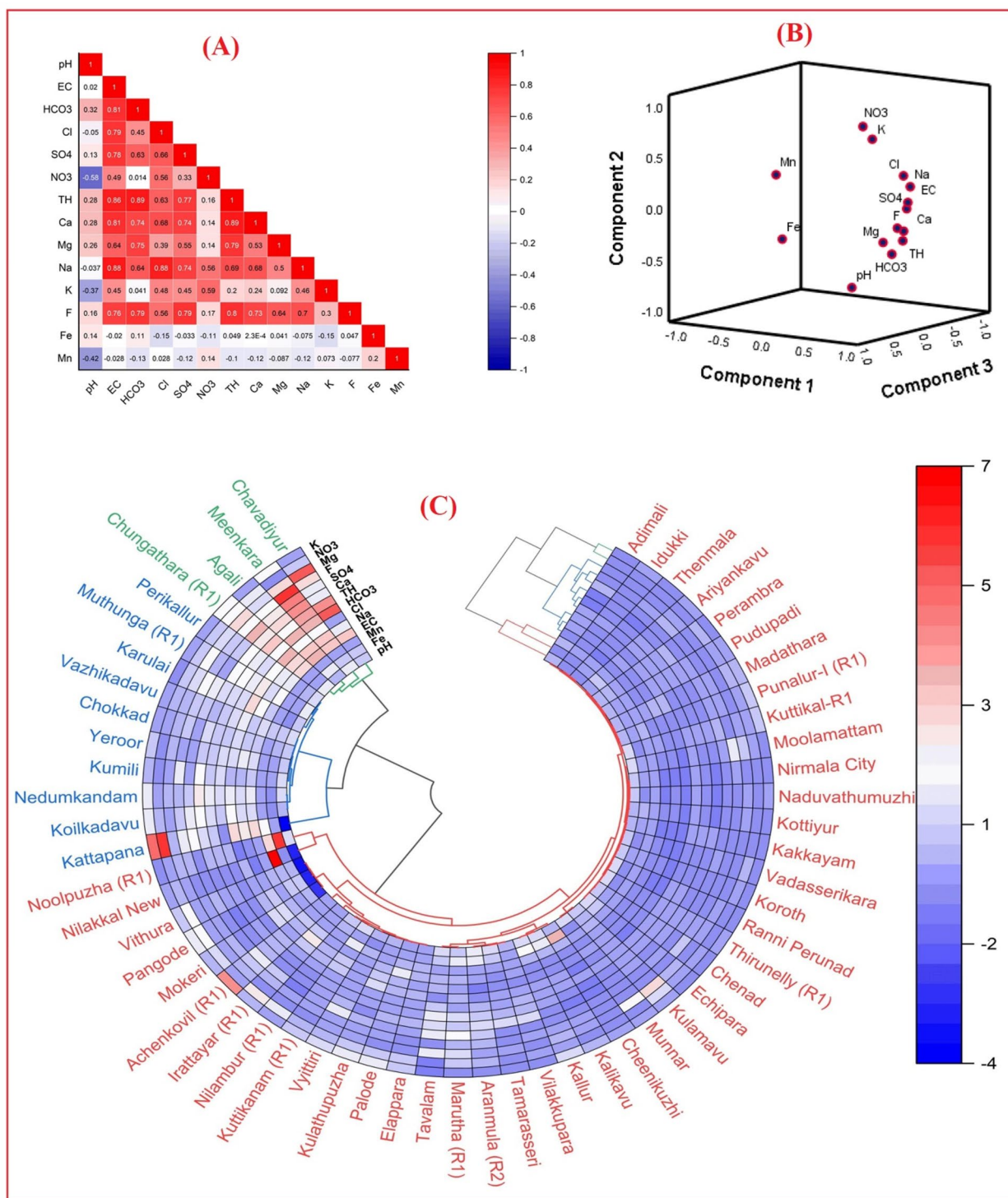


Figure 8. Multivariate statistical analysis. (A) Results of Pearson correlation analysis, (B) Results of Principle component analysis, (C) Results of Hierarchical cluster analysis in polar heat-map. The polar heat-map was generated using Originlab's, Origin 2022 for Desktop software (<https://www.originlab.com/origin>), version Origin Pro 2022.

Fe and Mn BIS drinking limits, respectively. WQI analysis revealed that a majority of the groundwater samples (68%) were classified as being within the excellent to good category for drinking purposes. Conversely, only 7% of the samples were deemed unfit for consumption owing to pollution from nitrates.

The predominant hydrochemical facies are CaHCO₃, followed by CaMgCl facies. Gibbs plots demonstrate that mineral weathering influences water chemistry. Alkaline earth metals exceed alkali metals in 72% of samples. About 47.4% are CaMgHCO₃ type, indicating direct recharge, while 26.3% are CaMgClSO₄ type, affected by

Component	Initial eigenvalues			Extraction sums of squared loadings		
	Total	% of variance	Cumulative %	Total	% of Variance	Cumulative %
1	7.032	50.227	50.227	7.032	50.227	50.227
2	2.510	17.931	68.158	2.510	17.931	68.158
3	1.260	9.001	77.159	1.260	9.001	77.159
4	0.743	5.304	82.463			
5	0.604	4.312	86.775			
6	0.547	3.908	90.683			
7	0.380	2.717	93.400			
8	0.283	2.025	95.425			
9	0.245	1.749	97.174			
10	0.164	1.169	98.343			
11	0.133	0.951	99.294			
12	0.051	0.364	99.658			
13	0.030	0.216	99.874			
14	0.018	0.126	100.000			

Table 2. Results of total variance in PCA. Extraction Method: Principal Component Analysis.

	Component		
	1	2	3
pH	0.135	-0.838	-0.187
EC	0.958	0.114	0.046
HCO ₃ ⁻	0.833	-0.393	0.137
Cl ⁻	0.802	0.338	-0.103
SO ₄ ²⁻	0.869	0.028	-0.061
NO ₃ ⁻	0.396	0.795	0.000
TH	0.926	-0.259	0.087
Ca ²⁺	0.866	-0.186	-0.014
Mg ²⁺	0.724	-0.291	0.128
Na ⁺	0.886	0.240	-0.097
K ⁺	0.421	0.655	-0.123
F ⁻	0.861	-0.142	0.085
Fe	-0.023	-0.242	0.758
Mn	-0.103	0.380	0.748

Table 3. Loading of Component matrix in PCA.

evaporation and gypsum. The presence of both types in the groundwater indicates temporary and permanent hardness. Silicate weathering is the primary source of elements in this aquifer, as shown by various molar ratios and plots. Water chemistry is mainly influenced by cation exchange and reverse ion processes. The dissolution of carbonate minerals (calcite, aragonite, dolomite, siderite, and rhodochrosite) and their supersaturation with hematite, goethite, and ferrihydrite influence groundwater chemistry. High Fe (II) and Mn (II) levels raise the SI of siderite and rhodochrosite. These metals are limited by adsorption or co-precipitation with CaCO₃.

Pearson correlation analysis shows EC and TH are highly associated with all variables except NO₃⁻, K⁺, and pH. A strong correlation between NO₃⁻ and K⁺ suggests anthropogenic origins. The positive correlation between HCO₃⁻ and Cl⁻ indicates that wastewater recharge influences mineral weathering and increases its concentrations. The HCA analysis in R mode showed four groups, with Cluster 1 (EC, TH, Na⁺, Mg²⁺, Cl⁻, HCO₃⁻, and SO₄²⁻) showing the impact of silicate and carbonate weathering. Cluster 2 (NO₃⁻ and K⁺) indicates the influence of anthropogenic factors. Cluster 3 (pH only) is not affected by weathering or anthropogenic factors. Cluster 4 includes Fe and Mn, suggesting a separate origin for these variables. Q-mode HCA yielded 3 clusters, with Cluster 1 (75% of wells) having less mineralized groundwater, Cluster 2 indicating wells having more mineralized groundwater than Cluster 1 wells, and cluster 3 showing high mineralization with an EC of 900 µS/cm, average. In the same way, PCA results show that Factor 1 makes up half of all samples and shows mineral weathering. Factors 2 (17.9%) and 3 (9.0%), on the other hand, show human/agricultural impact and different sources for Fe and Mn. Overall, the study highlights the complex interplay of natural processes and human factors shaping water quality in the region, emphasizing the need for comprehensive management strategies to safeguard groundwater quality in this ecologically sensitive region.

Data availability

The authors declare that the data supporting the findings of this study are available within the paper and its Supplementary Information files. Should any raw data files be needed in another format they are available from the corresponding author upon reasonable request. Source data are provided with this paper.

Received: 3 March 2024; Accepted: 18 July 2024

Published online: 19 August 2024

References

- Abba, S. I. *et al.* Emerging evolutionary algorithm integrated with kernel principal component analysis for modeling the performance of a water treatment plant. *J. Water Process Eng.* **33**, 101081. <https://doi.org/10.1016/j.jwpe.2019.101081> (2020).
- Adimalla, N. & Taloor, A. K. Hydrogeochemical investigation of groundwater quality in the hard rock terrain of South India using Geographic Information System (GIS) and groundwater quality index (GWQI) techniques. *Groundw. Sustain. Dev.* **10**, 100288. <https://doi.org/10.1016/j.gsd.2019.100288> (2020).
- Alam, W., Singh, K. S., Gyanendra, Y., Laishram, R. J. & Nesa, N. Hydrogeochemical assessment of groundwater quality for few habitations of Chandel District, Manipur (India). *Appl. Water Sci.* **10**, 123. <https://doi.org/10.1007/s13201-020-01208-0> (2020).
- American public health association, American water works association, Water environment federation (Eds.). Standard methods for the examination of water and wastewater, 22nd ed. ed. American public health association, Washington (D.C.) (2012).
- Biswas, A. *et al.* Groundwater chemistry and redox processes: Depth dependent arsenic release mechanism. *Appl. Geochem.* **26**, 516–525. <https://doi.org/10.1016/j.apgeochem.2011.01.010> (2011).
- Brindha, K. & Elango, L. Cross comparison of five popular groundwater pollution vulnerability index approaches. *J. Hydrol.* **524**, 597–613. <https://doi.org/10.1016/j.jhydrol.2015.03.003> (2015).
- Bureau of Indian Standards. Indian standard drinkingwater specification (second revision), Bureau of Indian Standards (BIS) (2012).
- Cerling, T. E., Pederson, B. L. & Von Damm, K. L. Sodium-calcium ion exchange in the weathering of shales: Implications for global weathering budgets. *Geology* **17**, 552. [https://doi.org/10.1130/0091-7613\(1989\)017%3c0552:SCIEIT%3e2.3.CO;2](https://doi.org/10.1130/0091-7613(1989)017%3c0552:SCIEIT%3e2.3.CO;2) (1989).
- CGWB. Ground Water Resources of Kerala, March 2017. Ground Water Department, Government of Kerala & Central Ground Water Board, Government of India (2017).
- Chadha, D. K. A proposed new diagram for geochemical classification of natural waters and interpretation of chemical data. *Hydrogeol. J.* **7**, 431–439. <https://doi.org/10.1007/s100400050216> (1999).
- Deutsch, W. *Groundwater geochemistry: fundamentals and applications to contamination* (Lewis Publishers, 1997).
- Domenico, P. A. & Schwartz, F. W. *Physical and chemical hydrogeology* 2nd edn. (Wiley, 1998).
- Edmunds, W. M. & Shand, P. (eds) *Natural groundwater quality* 1st edn. (Wiley, Hoboken, 2008). <https://doi.org/10.1002/978144300345>.
- Elumalai, V., Nwabisa, D. P. & Rajmohan, N. Evaluation of high fluoride contaminated fractured rock aquifer in South Africa—Geochemical and chemometric approaches. *Chemosphere* **235**, 1–11. <https://doi.org/10.1016/j.chemosphere.2019.06.065> (2019).
- Elumalai, V. *et al.* Geochemical evolution and the processes controlling groundwater chemistry using ionic ratios, geochemical modelling and chemometric analysis in uMhlathuze catchment, KwaZulu-Natal South Africa. *Chemosphere* **312**, 137179. <https://doi.org/10.1016/j.chemosphere.2022.137179> (2023).
- Ewaid, S., Abed, S., Al-Ansari, N. & Salih, R. Development and evaluation of a water quality index for the Iraqi rivers. *Hydrology* **7**, 67. <https://doi.org/10.3390/hydrology7030067> (2020).
- Fankhauser, K. *et al.* Estimating groundwater use and demand in arid Kenya through assimilation of satellite data and in-situ sensors with machine learning toward drought early action. *Sci. Total Environ.* **831**, 154453. <https://doi.org/10.1016/j.scitotenv.2022.154453> (2022).
- Gaillardet, J., Dupré, B., Louvat, P. & Allègre, C. J. Global silicate weathering and CO₂ consumption rates deduced from the chemistry of large rivers. *Chem. Geol.* **159**, 3–30. [https://doi.org/10.1016/S0009-2541\(99\)00031-5](https://doi.org/10.1016/S0009-2541(99)00031-5) (1999).
- Gastmans, D., Chang, H. K. & Hutcheon, I. Groundwater geochemical evolution in the northern portion of the Guarani Aquifer System (Brazil) and its relationship to diagenetic features. *Appl. Geochem.* **25**, 16–33. <https://doi.org/10.1016/j.apgeochem.2009.09.024> (2010).
- Gaur, N. *et al.* Evaluation of water quality index and geochemical characteristics of surfacewater from Tawang India. *Sci. Rep.* **12**, 11698. <https://doi.org/10.1038/s41598-022-14760-3> (2022).
- Herrera, C. *et al.* Groundwater flow in a closed basin with a saline shallow lake in a volcanic area: Laguna Tuyajto, northern Chilean Altiplano of the Andes. *Sci. Total Environ.* **541**, 303–318. <https://doi.org/10.1016/j.scitotenv.2015.09.060> (2016).
- Hounslow, A. W. *Water quality data: analysis and interpretation* 1st edn. (CRC Press, Boca Raton, 2018). <https://doi.org/10.1201/9780203734117>.
- Jankowski, J. & Acworth, R. I. Impact of debris-flow deposits on hydrogeochemical processes and the development of dryland salinity in the Yass river catchment, New South Wales Australia. *Hydrogeol. J.* **5**, 71–88. <https://doi.org/10.1007/s100400050119> (1997).
- John David, H. Study and interpretation of the chemical characteristics of natural water. *US Geological Survey Water-Supply Paper 2254*, University of Virginia, Charlottesville 263. <https://doi.org/10.3133/wsp2254> (1985).
- Jones, S. & Rosen, M. Controls on the chemical composition of groundwater from alluvial aquifers in the Wanaka and Wakatipu basins, Central Otago, New Zealand. *Hydrogeol. J.* **6**, 264–281. <https://doi.org/10.1007/s100400050150> (1998).
- Khan, A., Khan, H. H. & Umar, R. Impact of land-use on groundwater quality: GIS-based study from an alluvial aquifer in the western Ganges basin. *Appl. Water Sci.* **7**, 4593–4603. <https://doi.org/10.1007/s13201-017-0612-7> (2017).
- Khan, A., Umar, R. & Khan, H. H. Significance of silica in identifying the processes affecting groundwater chemistry in parts of Kali watershed, Central Ganga Plain India. *Appl. Water Sci.* **5**, 65–72. <https://doi.org/10.1007/s13201-014-0164-z> (2015).
- Khan, A., Umar, R. & Khan, H. H. Hydrochemical characterization of groundwater in lower Kali watershed, Western Uttar Pradesh. *J. Geol. Soc. India* **86**, 195–210. <https://doi.org/10.1007/s12594-015-0299-z> (2015).
- Khan, H. H. & Khan, A. Groundwater-surface water interaction along river Kali, near Aligarh, India. *HydroResearch* **2**, 119–128. <https://doi.org/10.1016/j.hydres.2019.12.001> (2019).
- Khan, H. H., Khan, A., Ahmed, S. & Perrin, J. GIS-based impact assessment of land-use changes on groundwater quality: Study from a rapidly urbanizing region of South India. *Environ. Earth Sci.* **63**, 1289–1302. <https://doi.org/10.1007/s12665-010-0801-2> (2011).
- Khatri, N., Tyagi, S., Rawtani, D., Tharmavaram, M. & Kamboj, R. D. Analysis and assessment of ground water quality in Satlasana Taluka, Mehsana district, Gujarat, India through application of water quality indices. *Groundw. Sustain. Dev.* **10**, 100321. <https://doi.org/10.1016/j.gsd.2019.100321> (2020).
- Kuldip-Singh, H. & Dhanwinder-Singh, H. S. Geochemistry and assessment of hydrogeochemical processes in groundwater in the southern part of Bathinda district of Punjab, northwest India. *Environ. Earth Sci.* **64**, 1823–1833. <https://doi.org/10.1007/s12665-011-0989-9> (2011).

33. Mayo, A. L. & Loucks, M. D. Solute and isotopic geochemistry and ground water flow in the central Wasatch Range. *Utah. J. Hydrol.* **172**, 31–59. [https://doi.org/10.1016/0022-1694\(95\)02748-E](https://doi.org/10.1016/0022-1694(95)02748-E) (1995).
34. McLean, J., Sililo, O., International Association of Hydrogeologists (Eds.), Groundwater, past achievements and future challenges: proceedings of the XXX IAH Congress on Groundwater Past Achievements and Future Challenges, Cape Town, South Africa, 26 November–1 December 2000. A.A. Balkema, Rotterdam, Netherlands ; Brookfield VT (2000).
35. Menberu, Z., Mogesse, B. & Reddythota, D. Evaluation of water quality and eutrophication status of Hawassa Lake based on different water quality indices. *Appl. Water Sci.* **11**, 61. <https://doi.org/10.1007/s13201-021-01385-6> (2021).
36. Meybeck, M. Global chemical weathering of surficial rocks estimated from river dissolved loads. *Am. J. Sci.* **287**, 401–428. <https://doi.org/10.2475/ajs.287.5.401> (1987).
37. Middelburg, J. J., De Lange, G. J. & Van Der Weijden, C. H. Manganese solubility control in marine pore waters. *Geochim. Cosmochim. Acta* **51**, 759–763. [https://doi.org/10.1016/0016-7037\(87\)90086-X](https://doi.org/10.1016/0016-7037(87)90086-X) (1987).
38. Moral, F., Cruz-Sanjulián, J. J. & Ollás, M. Geochemical evolution of groundwater in the carbonate aquifers of Sierra de Segura (Betic Cordillera, southern Spain). *J. Hydrol.* **360**, 281–296. <https://doi.org/10.1016/j.jhydrol.2008.07.012> (2008).
39. Nagaraju, A., Muralidhar, P. & Sreedhar, Y. Hydrogeochemistry and groundwater quality assessment of Rapur Area, Andhra Pradesh, South India. *J. Geosci. Environ. Prot.* **04**, 88–99. <https://doi.org/10.4236/gep.2016.44012> (2016).
40. Parkhurst, D.L., Appelo, C.A.J. Description of input and examples for PHREEQC version 3: a computer program for speciation, batch-reaction, one-dimensional transport, and inverse geochemical calculations., in: Modeling Techniques. U.S. Geological Survey, Denver, CO, p. 497, (2013).
41. Parkhurst, D.L., Appelo, C.A.J., 1999. User's guide to PHREEQC (Version 2): A computer program for speciation, batch-reaction, one-dimensional transport, and inverse geochemical calculations.
42. Pool, S. *et al.* Hydrological modeling of the effect of the transition from flood to drip irrigation on groundwater recharge using multi-objective calibration. *Water Resour. Res.* **57**, e2021WR029677. <https://doi.org/10.1029/2021WR029677> (2021).
43. Rajesh, R., Brindha, K. & Elango, L. Groundwater quality and its hydrochemical characteristics in a shallow weathered rock aquifer of Southern India. *Water Qual. Expo. Health* **7**, 515–524. <https://doi.org/10.1007/s12403-015-0166-6> (2015).
44. Rajmohan, N. & Elango, L. Identification and evolution of hydrogeochemical processes in the groundwater environment in an area of the Palar and Cheyyar River Basins, Southern India. *Environ. Geol.* **1**, 1–1. <https://doi.org/10.1007/s00254-004-1012-5> (2004).
45. Rajmohan, N., Masoud, M. H. Z. & Niyazi, B. A. M. Impact of evaporation on groundwater salinity in the arid coastal aquifer. *Western Saudi Arabia. CATENA* **196**, 104864. <https://doi.org/10.1016/j.catena.2020.104864> (2021).
46. Rajmohan, N., Patel, N., Singh, G. & Amarasinghe, U. A. Hydrochemical evaluation and identification of geochemical processes in the shallow and deep wells in the Ramganga Sub-Basin. *India. Environ. Sci. Pollut. Res.* **24**, 21459–21475. <https://doi.org/10.1007/s11356-017-9704-z> (2017).
47. Ram, A. *et al.* Groundwater quality assessment using water quality index (WQI) under GIS framework. *Appl. Water Sci.* **11**, 46. <https://doi.org/10.1007/s13201-021-01376-7> (2021).
48. Saha, A., Pal, S. C., Chowdhuri, I., Roy, P. & Chakraborty, R. Effect of hydrogeochemical behavior on groundwater resources in the Holocene aquifers of moribund Ganges Delta, India: Infusing data-driven algorithms. *Environ. Pollut.* **314**, 120203. <https://doi.org/10.1016/j.envpol.2022.120203> (2022).
49. Saikrishna, K. *et al.* Deciphering groundwater quality, mechanisms controlling groundwater chemistry in and around Suryapet, Telangana South India. *Total Environ. Res. Themes* **6**, 100035. <https://doi.org/10.1016/j.totert.2023.100035> (2023).
50. Schoeller, *Qualitative evaluation of groundwater resources* 5483 (UNESCO, 1965).
51. Şener, Ş., Şener, E. & Davraz, A. Evaluation of water quality using water quality index (WQI) method and GIS in Aksu River (SW-Turkey). *Sci. Total Environ.* **584–585**, 131–144. <https://doi.org/10.1016/j.scitotenv.2017.01.102> (2017).
52. Siraj, G., Khan, H. H. & Khan, A. Dynamics of surface water and groundwater quality using water quality indices and GIS in river Tamsa (Tons), Jalalpur, India. *HydroResearch* **6**, 89–107. <https://doi.org/10.1016/j.hydres.2023.02.002> (2023).
53. Somers, L. D. & McKenzie, J. M. A review of groundwater in high mountain environments. *WIREs Water* **7**, E1475. <https://doi.org/10.1002/wat2.1475> (2020).
54. Sreedevi, P. D., Srekanth, P. D., Ahmed, S. & Reddy, D. V. Evaluation of groundwater quality for irrigation in a semi-arid region of South India. *Sustain. Water Resour. Manag.* **5**, 1043–1056. <https://doi.org/10.1007/s40899-018-0279-8> (2019).
55. Sreedevi, P. D., Srekanth, P. D., Ahmed, S. & Reddy, D. V. Appraisal of groundwater quality in a crystalline aquifer: A chemometric approach. *Arab. J. Geosci.* **11**, 211. <https://doi.org/10.1007/s12517-018-3480-z> (2018).
56. Sreedevi, P. D., Srekanth, P. D., Khan, H. H. & Ahmed, S. Drainage morphometry and its influence on hydrology in an semi arid region: Using SRTM data and GIS. *Environ. Earth Sci.* **70**, 839–848. <https://doi.org/10.1007/s12665-012-2172-3> (2013).
57. Subba Rao, N., Dinakar, A., Kumari, B. K., Karunanidhi, D. & Kamalesh, T. Seasonal and spatial variation of groundwater quality vulnerable zones of yellareddygudem watershed, Nalgonda District, Telangana State India. *Arch. Environ. Contam. Toxicol.* **80**, 11–30. <https://doi.org/10.1007/s00244-020-00783-2> (2021).
58. Sunitha, V., Reddy, Y. S., Suvarna, B. & Reddy, B. M. Human health risk assessment (HHRA) of fluoride and nitrate using pollution index of groundwater (PIG) in and around hard rock terrain of Cuddapah, A.P South India. *Environ. Chem. Ecotoxicol.* **4**, 113–123. <https://doi.org/10.1016/j.enceco.2021.12.002> (2022).
59. Sunitha, V. & Sudharshan Reddy, Y. Hydrogeochemical evaluation of groundwater in and around Lakkireddipalli and Ramapuram, Y.S.R District, Andhra Pradesh India. *HydroResearch* **2**, 85–96. <https://doi.org/10.1016/j.hydres.2019.11.008> (2019).
60. Taylor, R. G. & Howard, K. W. F. Groundwater recharge in the Victoria Nile basin of east Africa: Support for the soil moisture balance approach using stable isotope tracers and flow modelling. *J. Hydrol.* **180**, 31–53. [https://doi.org/10.1016/0022-1694\(95\)02899-4](https://doi.org/10.1016/0022-1694(95)02899-4) (1996).
61. Tian, Y. *et al.* Using a water quality index to assess the water quality of the upper and middle streams of the Luanhe River, northern China. *Sci. Total Environ.* **667**, 142–151. <https://doi.org/10.1016/j.scitotenv.2019.02.356> (2019).
62. Todd, D. K. & Mays, L. W. *Groundwater hydrology* 3rd edn. (J. Wiley, 2005).
63. Tripathi, M. & Singal, S. K. Use of principal component analysis for parameter selection for development of a novel water quality index: A case study of river Ganga India. *Ecol. Indic.* **96**, 430–436. <https://doi.org/10.1016/j.ecolind.2018.09.025> (2019).
64. Tripti, M., Lambs, L., Moussa, I. & Corenblit, D. Evidence of elevation effect on stable isotopes of water along highlands of a humid tropical mountain belt (Western Ghats, India) experiencing monsoonal climate. *J. Hydrol.* **573**, 469–485. <https://doi.org/10.1016/j.jhydrol.2019.03.086> (2019).
65. Welch, A. H. & Lico, M. S. Factors controlling As and U in shallow ground water, southern Carson Desert Nevada. *Appl. Geochem.* **13**, 521–539. [https://doi.org/10.1016/S0883-2927\(97\)00083-8](https://doi.org/10.1016/S0883-2927(97)00083-8) (1998).
66. World Health Organization, 2017. Guidelines for drinking-water quality: fourth edition incorporating first addendum, 4th ed + 1st add. ed. World Health Organization, Geneva.
67. Yenugu, S. R., Vangala, S. & Badri, S. Monitoring of groundwater quality for drinking purposes using the WQI method and its health implications around inactive mines in Vemula-Vempalli region, Kadapa District South India. *Appl. Water Sci.* **10**, 202. <https://doi.org/10.1007/s13201-020-01284-2> (2020).
68. Yousefi, M. *et al.* Data on microbiological quality assessment of rural drinking water supplies in Poldasht county. *Data Brief* **17**, 763–769. <https://doi.org/10.1016/j.dib.2018.02.003> (2018).

69. Zaidi, F. K., Nazzal, Y., Jafri, M. K., Naeem, M. & Ahmed, I. Reverse ion exchange as a major process controlling the groundwater chemistry in an arid environment: a case study from northwestern Saudi Arabia. *Environ. Monit. Assess.* **187**, 607. <https://doi.org/10.1007/s10661-015-4828-4> (2015).
70. Zhang, C. & Selinus, O. Statistics and GIS in environmental geochemistry—Some problems and solutions. *J. Geochem. Explor.* **64**, 339–354. [https://doi.org/10.1016/S0375-6742\(98\)00048-X](https://doi.org/10.1016/S0375-6742(98)00048-X) (1998).

Acknowledgements

The authors express sincere thanks to the CGWB, KR, Trivandrum and PGTD (Chemistry) RTMNU, Nagpur for the facilities extended towards publication of this paper. The ideology addressed in this paper solely belongs to the authors only and not necessarily of their organizations.

Author contributions

PB contributed to the study's design, conceptualization, sample analysis, validation, methodology development, software implementation, statistical analysis, and was responsible for writing the original draft as well as reviewing and editing the manuscript. MC provided supervision throughout the study, contributed to data visualization, and participated in reviewing and editing the manuscript. BJV was involved in refining the methodology, contributed to writing, reviewing, and editing the manuscript, and provided supervision. AKN conducted field investigations, collected samples, and performed sample analysis. RJ contributed to conceptualization, methodology development, software implementation, statistical analysis, and participated in writing, reviewing, and editing the manuscript.

Competing interests

The authors declare no competing interests.

Additional information

Supplementary Information The online version contains supplementary material available at <https://doi.org/10.1038/s41598-024-67988-6>.

Correspondence and requests for materials should be addressed to P.B.

Reprints and permissions information is available at www.nature.com/reprints.

Publisher's note Springer Nature remains neutral with regard to jurisdictional claims in published maps and institutional affiliations.



Open Access This article is licensed under a Creative Commons Attribution-NonCommercial-NoDerivatives 4.0 International License, which permits any non-commercial use, sharing, distribution and reproduction in any medium or format, as long as you give appropriate credit to the original author(s) and the source, provide a link to the Creative Commons licence, and indicate if you modified the licensed material. You do not have permission under this licence to share adapted material derived from this article or parts of it. The images or other third party material in this article are included in the article's Creative Commons licence, unless indicated otherwise in a credit line to the material. If material is not included in the article's Creative Commons licence and your intended use is not permitted by statutory regulation or exceeds the permitted use, you will need to obtain permission directly from the copyright holder. To view a copy of this licence, visit <http://creativecommons.org/licenses/by-nc-nd/4.0/>.

© The Author(s) 2024